

## Supporting Information

### Vapochromic Separation of Toluene and Pyridine Azeotropes by Adaptive Macrocycle Co-Crystals

*Bin Li,\* Yun Wang, Yuan Wang, Yue Liu, Lu Wang, Zhi-Yuan Zhang and Chunju Li.\**

*Academy of Interdisciplinary Studies on Intelligent Molecules, Tianjin Key Laboratory of Structure and Performance for Functional Molecules, College of Chemistry, Tianjin Normal University, Tianjin 300387, P. R. China.*

Corresponding author. E-mail: bli@tjnu.edu.cn; cjli@shu.edu.cn

### Contents

|  |     |
|--|-----|
| 1. Materials and methods                             | S2  |
| 2. Characteristics of Dioxane@P5-PDI co-crystals     | S3  |
| 3. Characterization of P5-PDI $\alpha$ materials     | S7  |
| 4. Single-component solid-vapor sorption experiments | S9  |
| 5. Crystal engineering of Py@P5-PDI Co-crystals      | S14 |
| 6. Two-component solid-vapor sorption experiments    | S16 |
| 7. References  | S18 |

## 1. Materials and methods

Toluene and pyridine were purchased from Adamas-beta Chemical Company without further purification. Per-ethylated pillar[5]arene (P5) and N,N'-bis(*n*-butyl)pyromellitic diimide (PDI) were prepared according to literature procedures.<sup>[S1,S2]</sup> <sup>1</sup>H NMR spectra were recorded using a Bruker Avance 400 MHz spectrometer. Single crystal X-ray diffraction data of Dioxane@P5-PDI was collected on a Bruker D8-Venture detector using Mo-K $\alpha$  radiation ( $\lambda = 0.71073$  Å), and Py@P5-PDI was collected on a Bruker APEX-II CCD detector using Ga-K $\alpha$  radiation ( $\lambda = 1.34139$  Å). The crystal structure was solved and refined against all  $F^2$  values using the SHELX and Olex 2 suite of programs.<sup>[S3,S4]</sup> Diffuse reflectance spectra were recorded on a Shimadzu UV-3600i Plus spectrometer. Thermogravimetric Analysis (TGA) was recorded using a TA Instrument TA-Q500 and the samples were heated under nitrogen gas at a rate of 10 °C /min. Powder X-ray diffraction (PXRD) data were measured with a powder X-ray diffractometer (D/max 2200vpc, Rigaku, Japan) using Cu K $\alpha$  radiation ( $\lambda = 1.5046$  Å) with a range 5–40 °C. Head Space Gas Chromatographic (HS-GC) measurement was carried out using an Agilent 7890B instrument configured with an FID detector.

**Sample preparation of P5-PDI $\alpha$ .** P5 (3.0 g) was first of all mixed with PDI (0.75 g) in dioxane (30 mL) and dissolved by ultrasonic treatment. The solution was filtered with a 0.22- $\mu$ m syringe filter. Then slow evaporation of the solvent within 5 days afforded orange co-crystals of Dioxane@P5-PDI. The resulting co-crystals were further activated under vacuum at 75 °C for 12 h to obtain solvent-free crystalline materials of P5-PDI $\alpha$ .

**Co-crystal growth of Py@P5-PDI.** Co-crystals of Py@P5-PDI were grown by slow evaporation of a pyridine solution (1 mL) of P5 (20 mg) and PDI (6.0 mg) at room temperature. After a week, yellow co-crystals suitable for X-ray structural determination were obtained.

**Vaporhromic experiments.** An open 2 mL vial containing 10 mg of P5-PDI $\alpha$  was placed in a sealed 20 mL vial containing 1 mL of Py or Tol or Py/Tol mixture (*v/v* 50:50). P5-PDI $\alpha$  materials were exposed under saturated vapor pressure in the closed vessel at room temperature. Obvious naked-eye color changes could be observed over the time.

## 2. Characteristics of Dioxane@P5-PDI co-crystals

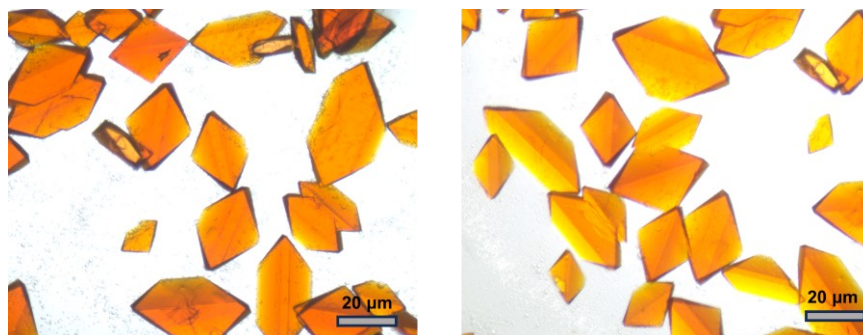


**Figure S1.** Photographs of the crystal growth of Dioxane@P5-PDI by slow evaporation of a solution of P5 and PDI in dioxane. Scale bar: 20  $\mu\text{m}$ .

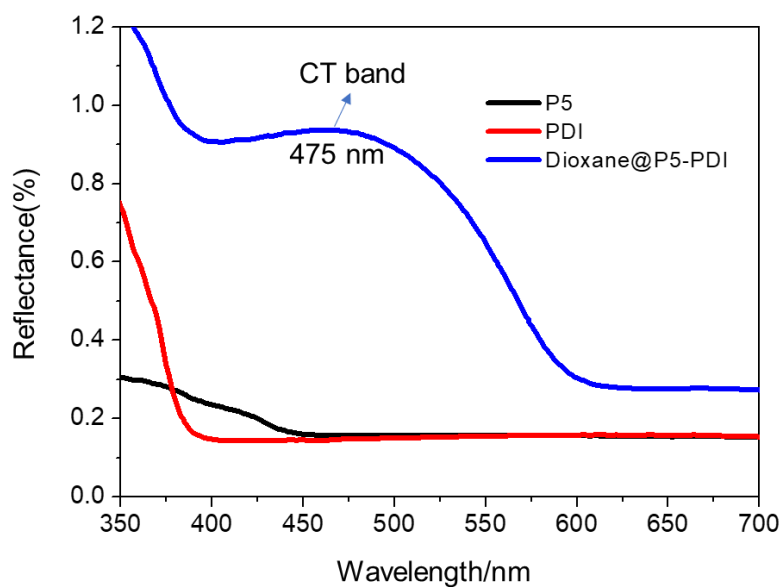


**Figure S2.** Diffuse reflectance spectra of individual P5 and PDI, and Dioxane@P5-PDI co-crystals. An obvious absorption at 475 nm was observed in Dioxane@P5-PDI, indicating the formation of CT complex between P5 and PDI.

**Table S1.** Crystal data and structure refinement for Dioxane@P5-PDI.

| Formula                                      | Dioxane@P5-PDI   |
|--|--|
| Crystallization solvent                      | Dioxane  |
| Formula                                      | C <sub>8</sub> H <sub>106</sub> N <sub>2</sub> O <sub>18</sub> |
| Formula weight                               | 1395.67  |
| Temperature / K                              | 100  |
| Crystal system                               | Monoclinic   |
| Space group                                  | <i>P2<sub>1</sub>/c</i>  |
| a / Å  | 12.3241(18)  |
| b / Å  | 33.684(6)  |
| c / Å  | 20.229(3)  |
| α / °  | 90   |
| β / °  | 96.013(4)  |
| γ / °  | 90   |
| Volume / Å <sup>3</sup>                      | 8351(2)  |
| Z  | 4  |
| ρ <sub>calc</sub> g/cm <sup>3</sup>          | 1.11   |
| μ / mm <sup>-1</sup>                         | 0.078  |
| Crystal size / mm <sup>3</sup>               | 0.14 × 0.12 × 0.09   |
| Radiation                                    | Mo-Kα (λ = 0.71073 Å)  |
| F(000)                                       | 3000.0   |
| 2θ range for data collection / °             | 3.898 to 55.022  |
| Index ranges                                 | -14 ≤ h ≤ 15, -43 ≤ k ≤ 43, -26 ≤ l ≤ 26                       |
| Reflections collected                        | 105718   |
| R <sub>int</sub>                             | 0.0911   |
| Goodness-of-fit on F <sup>2</sup>            | 1.013  |
| Final R <sub>1</sub> indexes [I ≥ 2σ(I)]     | 0.0616   |
| Final R <sub>1</sub> indexes [all data]      | 0.1246   |
| Final wR(F <sub>2</sub> ) indexes [all data] | 0.1750   |
| Largest diff. peak/hole / eÅ <sup>-3</sup>   | 0.30/-0.34   |
| <b>CCDC number</b>                           | <b>2340989</b>   |

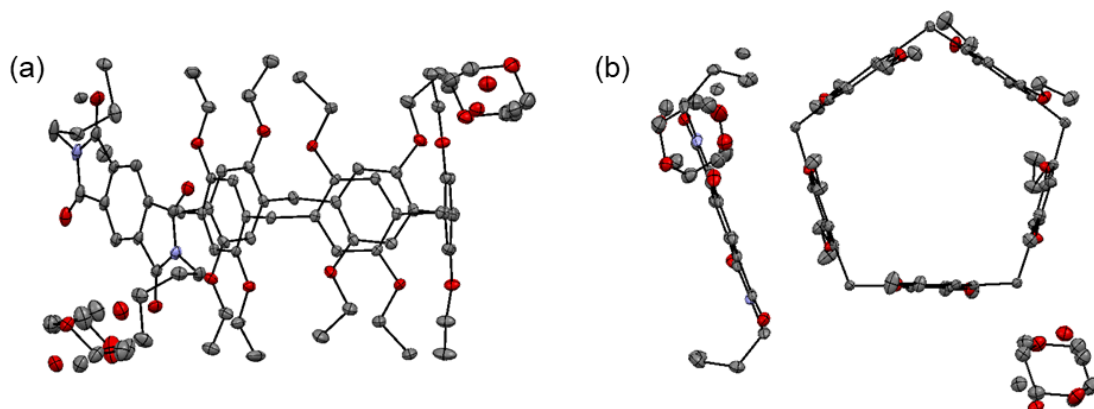


**Figure S3.** ORTEP drawing of Dioxane@P5-PDI with one P5, one PDI and two dioxane in the asymmetric unit from plane view (a) and side-on view (b). The thermal ellipsoids are displayed at a 30% probability. Hydrogen atoms have been omitted for clarity.

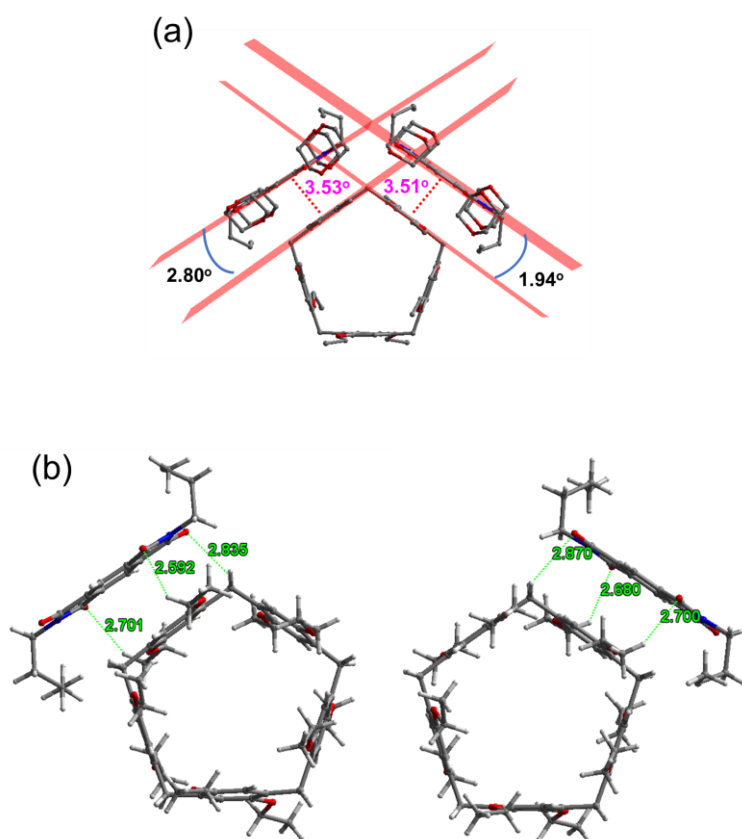


**Figure S4.** (a) The centroid–centroid distances [3.51 and 3.53 Å] and the dihedral angles [1.94° and 2.80°] of face-to-face  $\pi\cdots\pi$  interactions between adjacent P5 and PDI in the crystal structure of Dioxane@P5-PDI. (b) The C–H $\cdots$ O interactions [2.59–2.87 Å] between P5 and PDI.

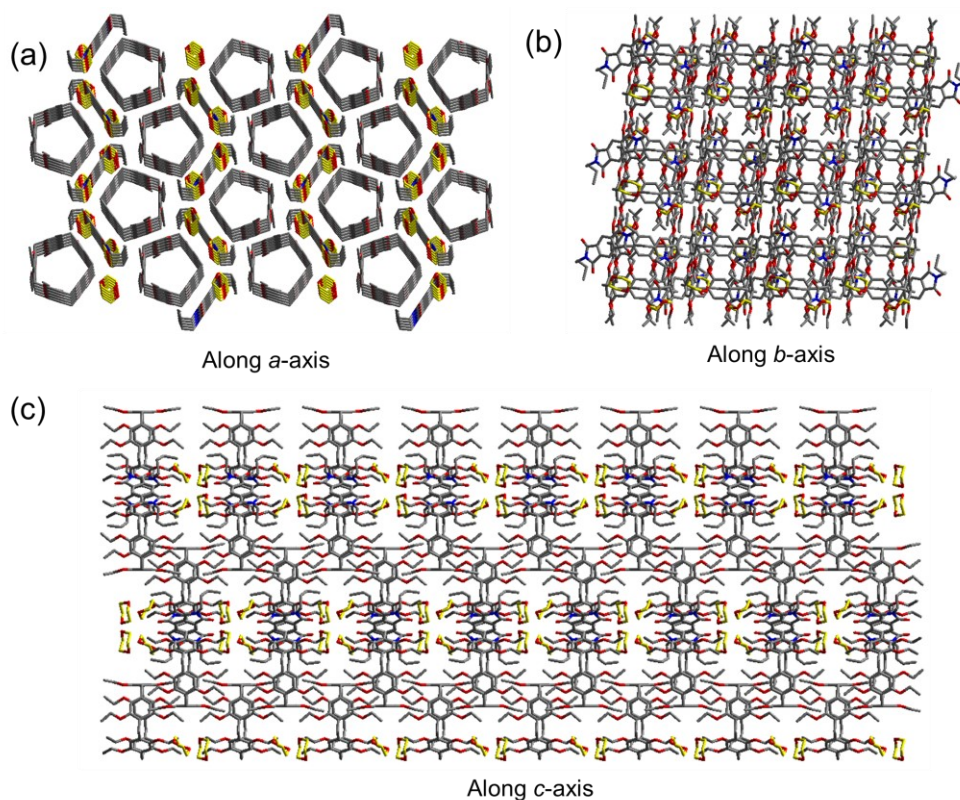


**Figure S5.** The packing modes of Dioxane@P5-PDI along the crystallographic *a*, *b*, and *c*-axis, respectively.

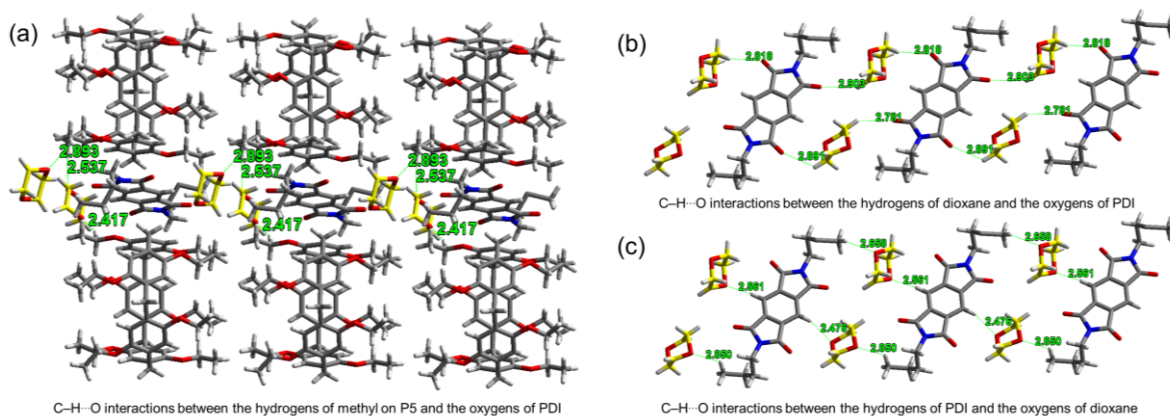


**Figure S6.** (a) The C-H...O interactions [2.42–2.89 Å] between the oxygens of dioxane and hydrogens of methyl on P5 in Dioxane@P5-PDI. (b) The C-H...O interactions [2.78–2.90 Å] between the hydrogens of dioxane and the oxygens of PDI in Dioxane@P5-PDI. (c) The C-H...O interactions [2.48–2.85 Å] between the oxygens of dioxane and the hydrogens of PDI.

### 3. Characterization of P5-PDI $\alpha$ materials

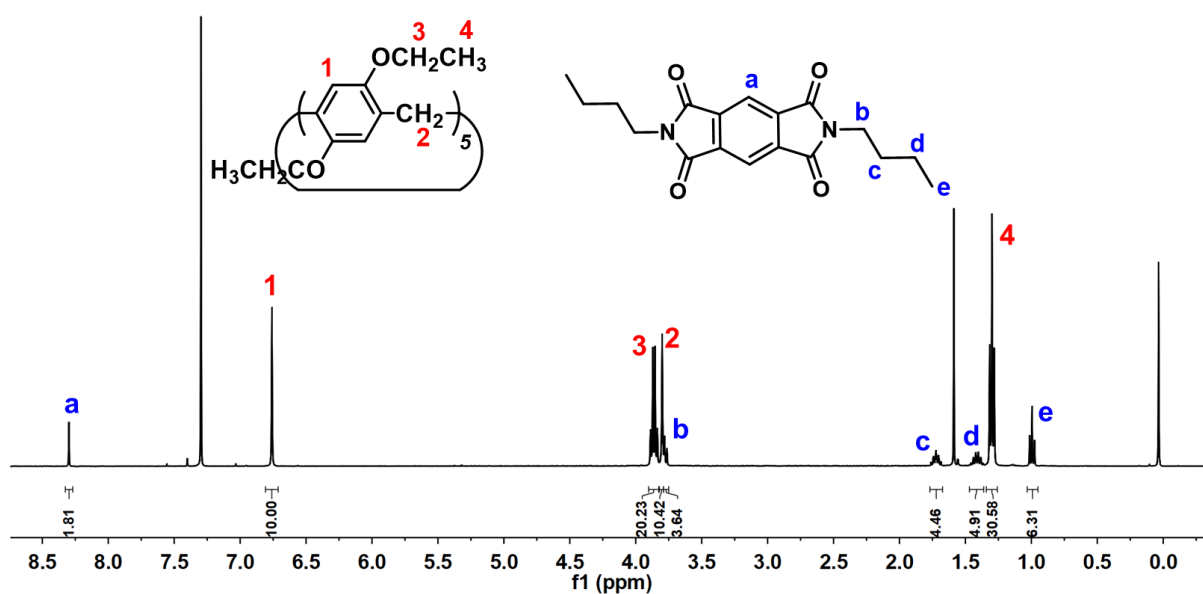


**Figure S7.** <sup>1</sup>H NMR spectrum (400 MHz, 298K, CDCl<sub>3</sub>) of P5-PDI $\alpha$ , showing a 1:1 stoichiometric ratio of P5 and PDI without any dioxane peaks.

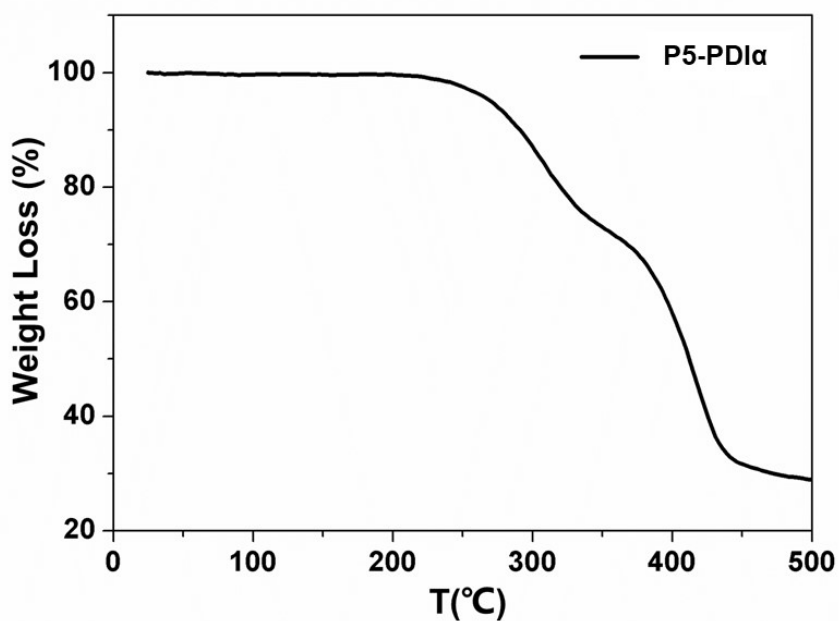


**Figure S8.** TGA curve of P5-PDI $\alpha$  recorded under a nitrogen atmosphere. Almost no weight loss occurs below 200 °C, supporting its high stability and the complete removal of solvents through activation.

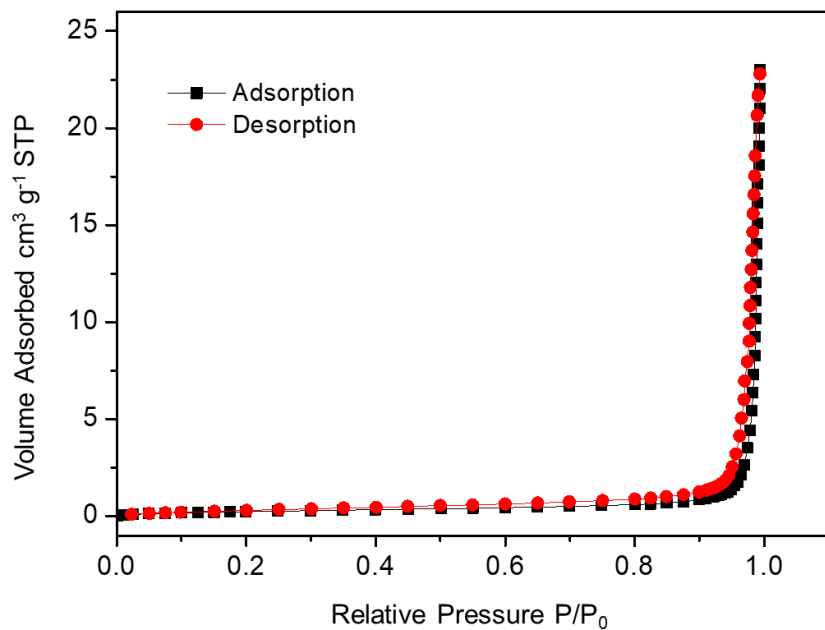


**Figure S9.** N<sub>2</sub> adsorption/desorption isotherm of P5-PDI $\alpha$ .



**Figure S10.** Color changes of P5-PDI $\alpha$  after adsorption of dioxane and Dioxane@P5-PDI after desorption of dioxane.

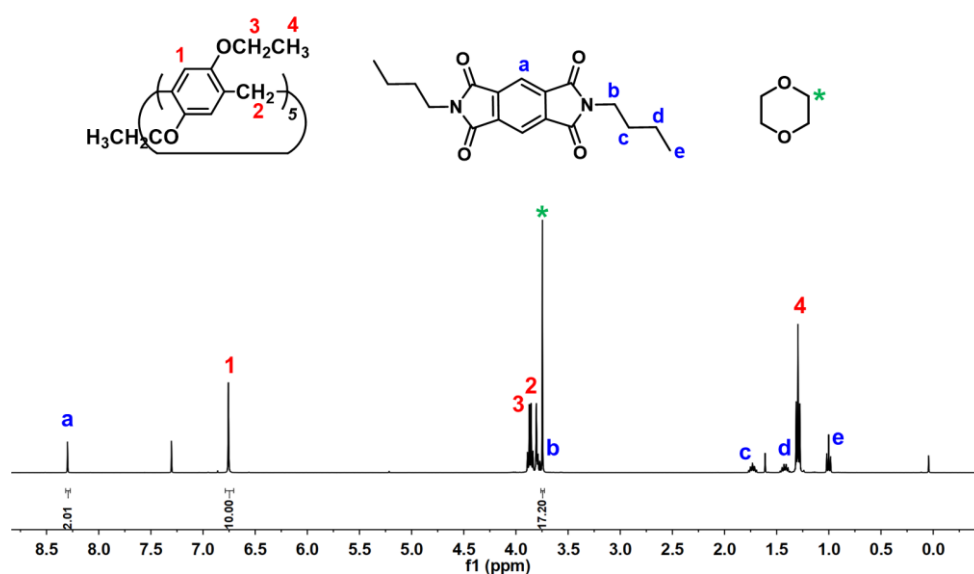


**Figure S11.** <sup>1</sup>H NMR spectrum (400MHz, 298K, CDCl<sub>3</sub>) of P5-PDI $\alpha$  after adsorption of dioxane.



#### 4. Single-component solid-vapor sorption experiments

For single-component Py or Tol adsorption experiment, an open 3 mL vial containing 5.0 mg of P5-PDI $\alpha$  adsorbent was placed in a sealed 20 mL vial containing 1 mL of Py or Tol. Uptake amount in the P5-PDI $\alpha$  crystals was monitored over time by  $^1\text{H}$  NMR spectra by completely dissolving the crystals in  $\text{CDCl}_3$ . Desorption experiments after uptake saturation were carried out by TGA analysis. The purity of Py was measured by GC. Before measurements, the crystals were heated at 30  $^\circ\text{C}$  to remove the surface-physically adsorbed vapor molecules.

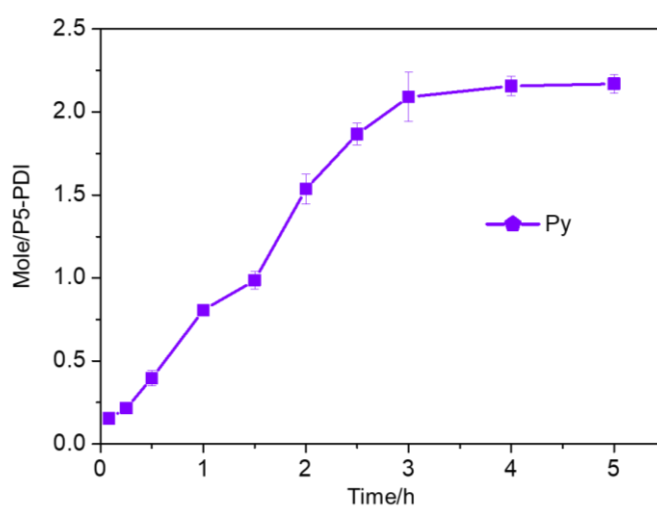


**Figure S12.** Time-dependent solid–vapor sorption plots of P5-PDI $\alpha$  for single-component Py vapor.

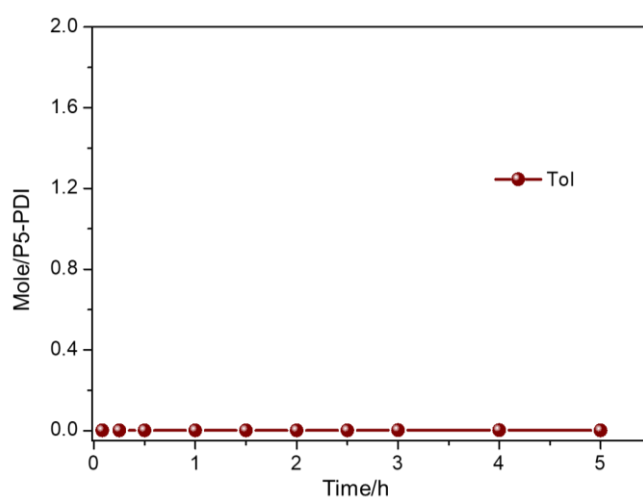


**Figure S13.** Time-dependent solid–vapor sorption plots of P5-PDI $\alpha$  for single-component Tol vapor. Absolutely no Tol was adsorbed.

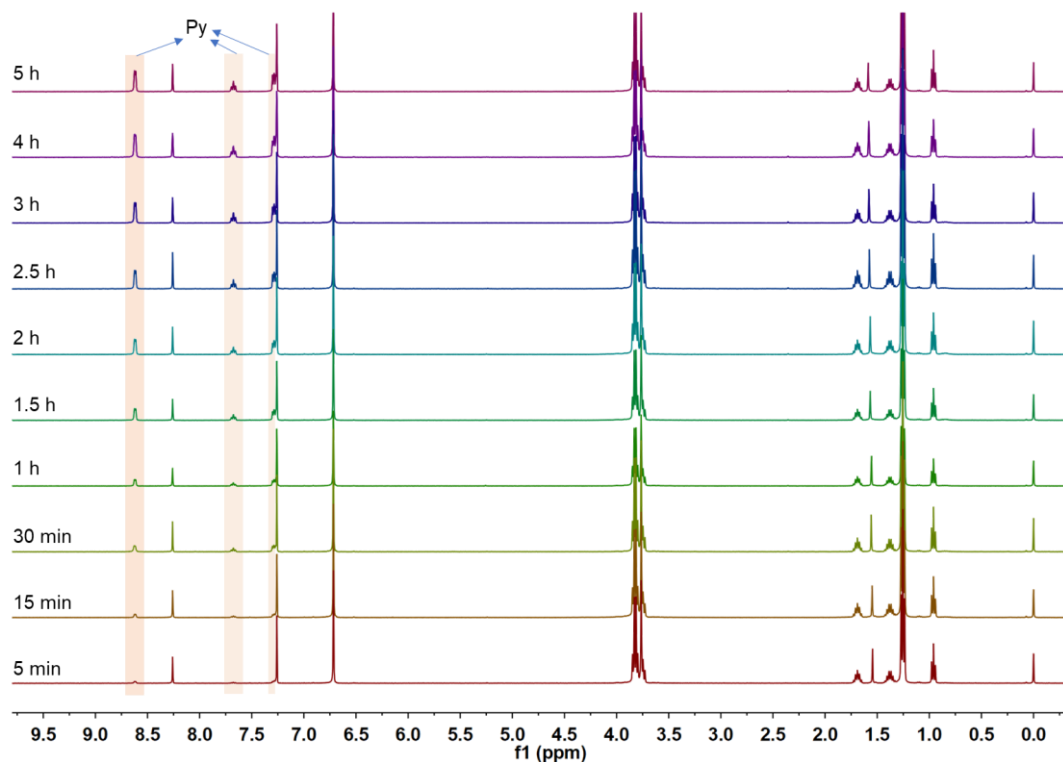


**Figure S14.** Time-dependent  $^1\text{H}$  NMR spectra (400 MHz, 298K,  $\text{CDCl}_3$ ) of P5-PDI $\alpha$  after uptake of Py vapor. The relative uptake of Py by P5-PDI $\alpha$  is plotted in Figure S12.

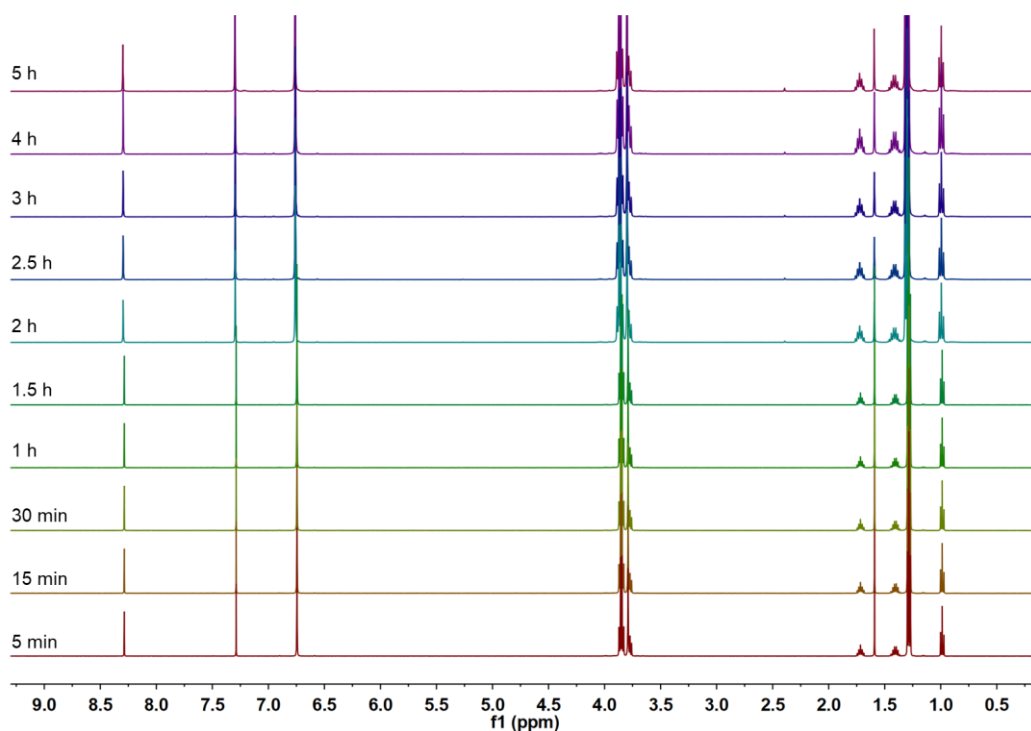


**Figure S15.** Time-dependent  $^1\text{H}$  NMR spectra (400 MHz, 298K,  $\text{CDCl}_3$ ) of P5-PDI $\alpha$  after uptake of Tol vapor. The relative uptake of Tol by P5-PDI $\alpha$  is plotted in Figure S13. Absolutely no Tol was adsorbed.



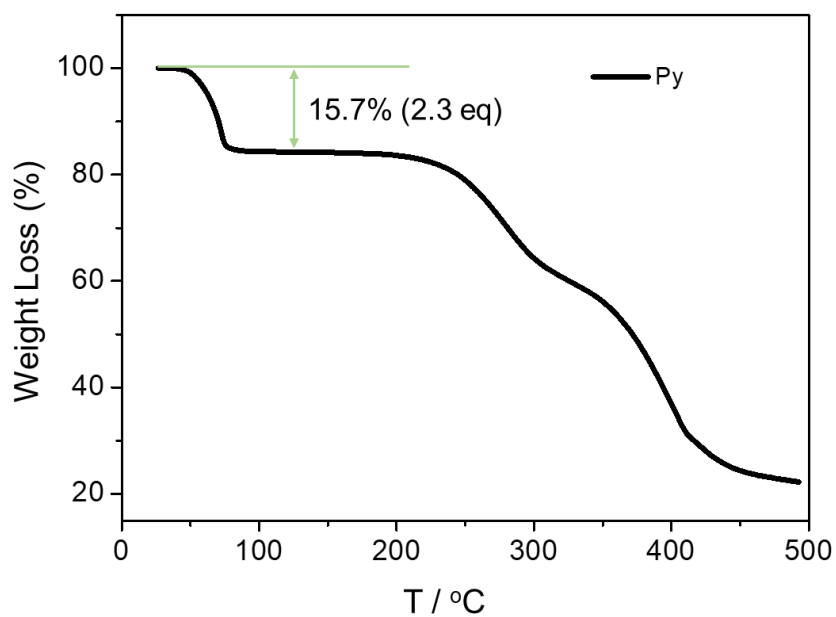


**Figure S18.** TGA profile of P5-PDI $\alpha$  after uptake of Py. About two Py molecules per P5-PDI were lost at 200 °C.

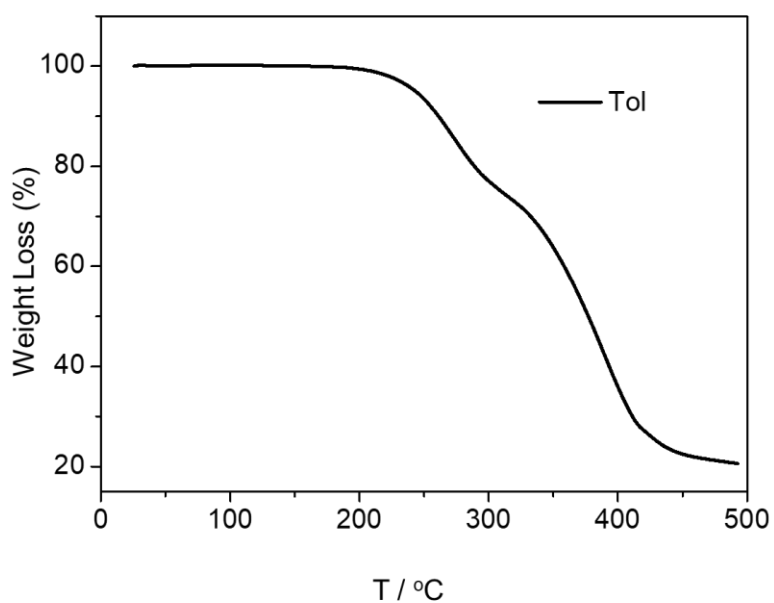


**Figure S19.** TGA profile of P5-PDI $\alpha$  after uptake of Tol. Almost no weight loss occurs below 200 °C, indicating no Tol is adsorbed.

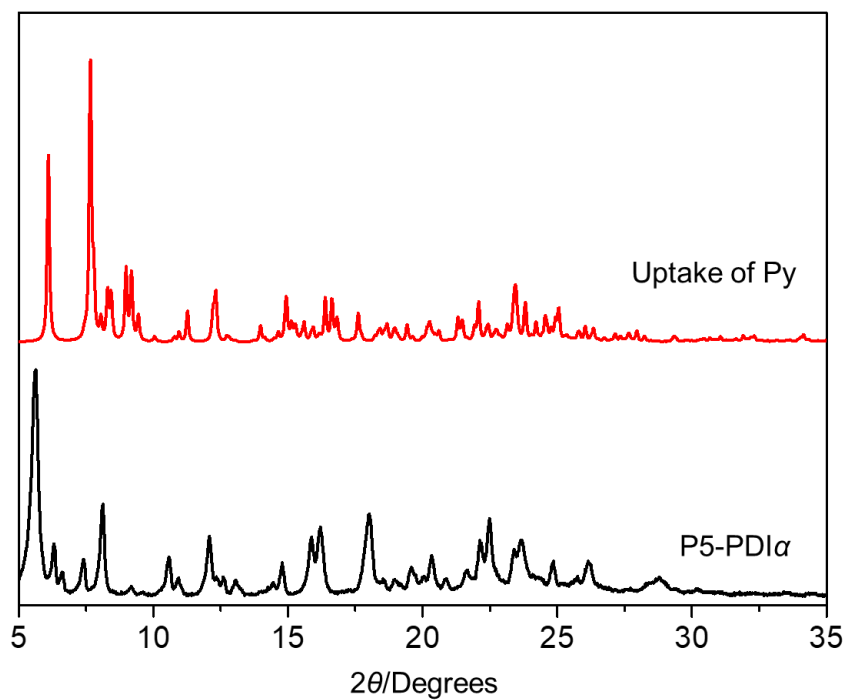


**Figure S20.** PXRD patterns of P5-PDI $\alpha$  before and after capture of Py.

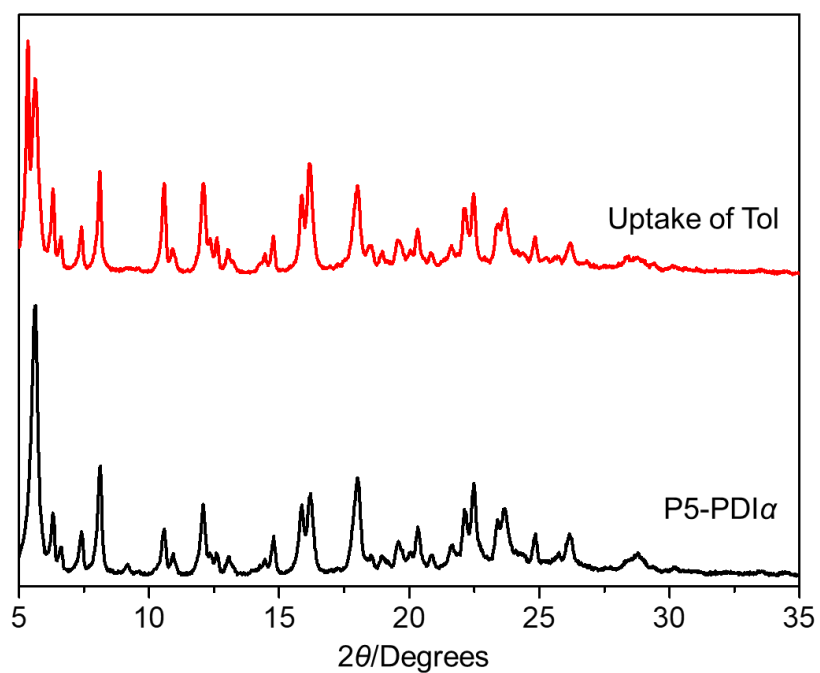


**Figure S21.** PXRD patterns of P5-PDI $\alpha$  before and after capture of Tol. No structural transformation was observed.

## 5. Crystal engineering of Py@P5-PDI co-crystals

**Table S2.** Crystal data and structure refinement for Py@P5-PDI.

| Formula   | Py@P5-PDI   |
|---|---|
| Crystallization solvent   | Pyridine  |
| Formula   | C <sub>93</sub> H <sub>110</sub> N <sub>6</sub> O <sub>14</sub> |
| Formula weight  | 1535.86   |
| Temperature / K   | 193.00  |
| Crystal system  | Triclinic   |
| Space group   | <i>P</i> -1   |
| <i>a</i> / Å  | 12.0800(5)  |
| <i>b</i> / Å  | 12.4509(5)  |
| <i>c</i> / Å  | 29.1324(11)   |
| $\alpha$ / °  | 94.272(2)   |
| $\beta$ / °   | 92.465(2)   |
| $\gamma$ / °  | 106.740(2)  |
| Volume / Å <sup>3</sup>   | 4174.8(3)   |
| <i>Z</i>  | 2   |
| $\rho_{\text{calc}}$ g/cm <sup>3</sup>                                    | 1.222   |
| $\mu$ / mm <sup>-1</sup>  | 0.419   |
| Crystal size / mm <sup>3</sup>  | 0.12 × 0.11 × 0.08  |
| Radiation   | Ga-K $\alpha$ ( $\lambda$ = 1.34139 Å)                          |
| F(000)  | 1476  |
| 2 $\Theta$ range for data collection / °                                  | 6.476 to 105.956  |
| Index ranges  | -14 ≤ <i>h</i> ≤ 14, -14 ≤ <i>k</i> ≤ 14, -34 ≤ <i>l</i> ≤ 34   |
| Reflections collected   | 54799   |
| <i>R</i> <sub>int</sub>   | 0.0482  |
| Goodness-of-fit on <i>F</i> <sup>2</sup>                                  | 1.179   |
| Final <i>R</i> <sub>1</sub> indexes [ <i>I</i> ≥ 2 $\sigma$ ( <i>I</i> )] | 0.0871  |
| Final <i>R</i> <sub>1</sub> indexes [all data]                            | 0.1358  |
| Final w <i>R</i> ( <i>F</i> <sub>2</sub> ) indexes [all data]             | 0.2856  |
| Largest diff. peak/hole / eÅ <sup>-3</sup>                                | 0.77/-0.75  |
| <b>CCDC number</b>  | <b>2340990</b>  |

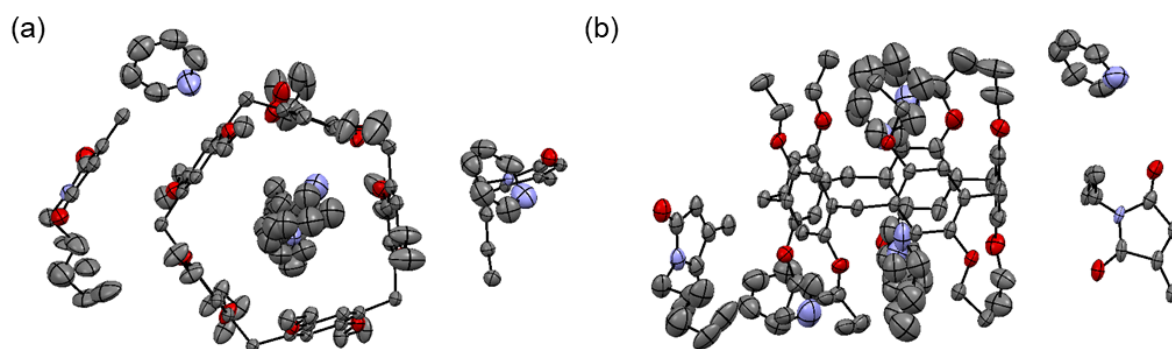


**Figure S22.** ORTEP drawing of Py@P5-PDI with one P5, one PDI (with occupancy factor of 0.5) and four Py in the asymmetric unit from plane view (a) and side-on view (b). The thermal ellipsoids are displayed at a 30% probability. Hydrogen atoms have been omitted for clarity.

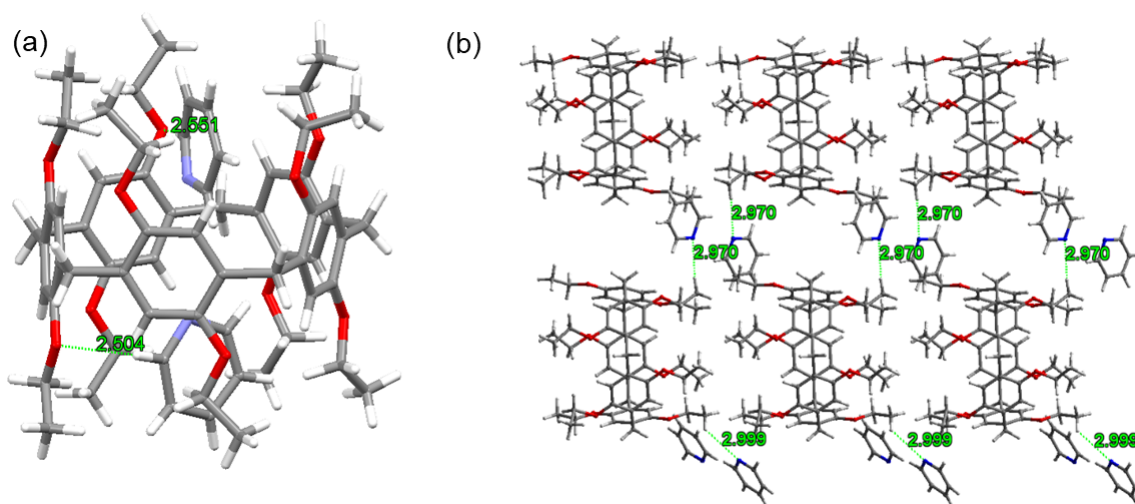


**Figure S23** (a) C–H···O interactions [2.55 and 2.50 Å] between P5 and Py contained in P5 cavity. (b) C–H···N interactions [2.97 and 3.00 Å] between P5 and outside Py in the crystal structure of Py@P5-PDI. The PDI molecules are omitted for clarity.

## 6. Two-component solid-vapor sorption experiments

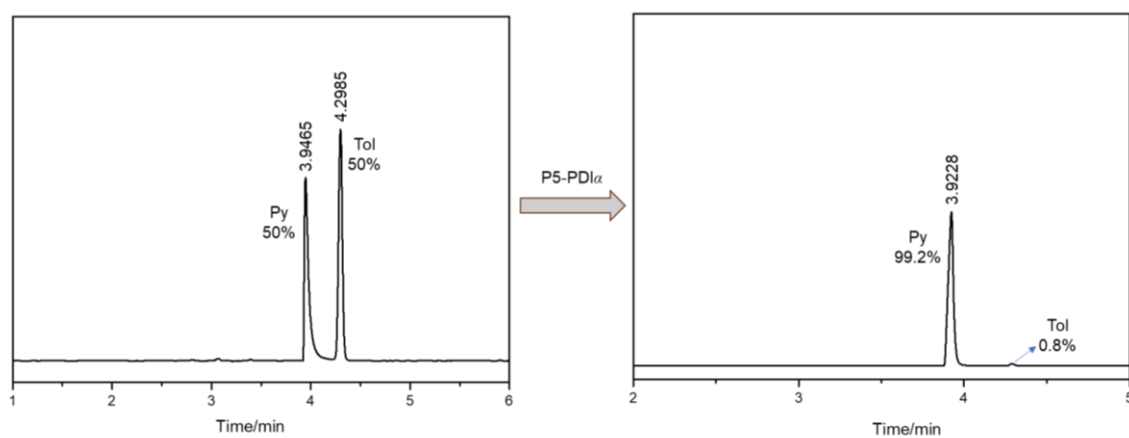


**Figure S24.** Relative Py and Tol uptake in P5-PDI $\alpha$  after saturation using GC.

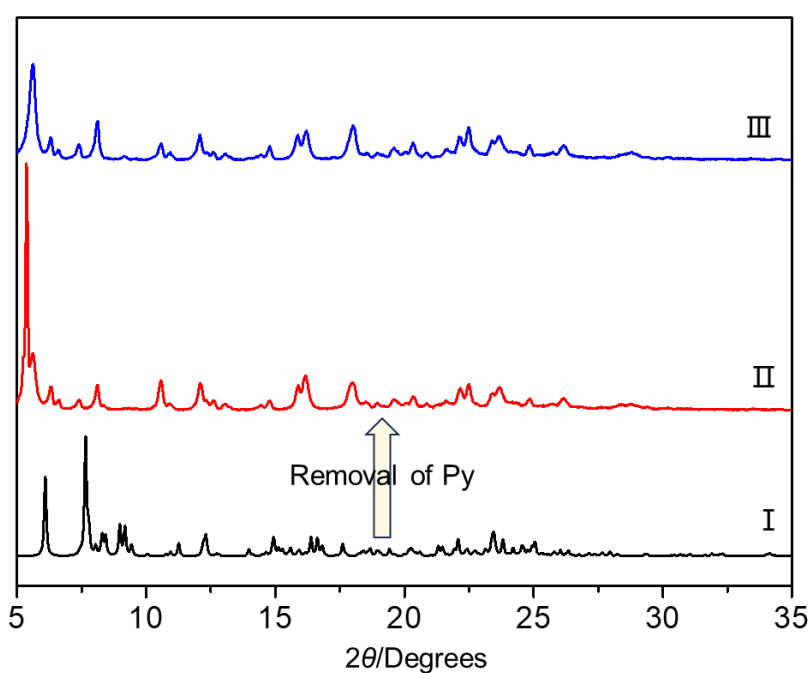


**Figure S25.** PXRD patterns of P5-PDI: (I) Py@P5-PDI; (II) after release of Py upon heating. (III) P5-PDI $\alpha$ . The results showed the structure of Py@P5-PDI transform back to the original structure of P5-PDI $\alpha$  after removing Py upon heating.



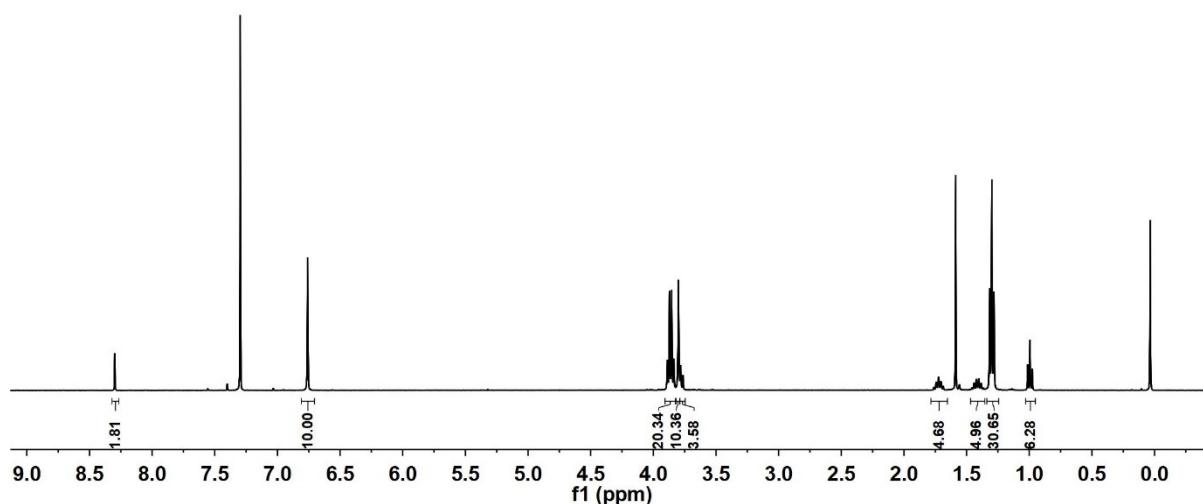


**Figure S26.**  $^1\text{H}$  NMR spectrum (400MHz, 298K,  $\text{CDCl}_3$ ) of  $\text{Py}@P5\text{-PDI}$  after desorption of Py by heating. No Py peaks were found.

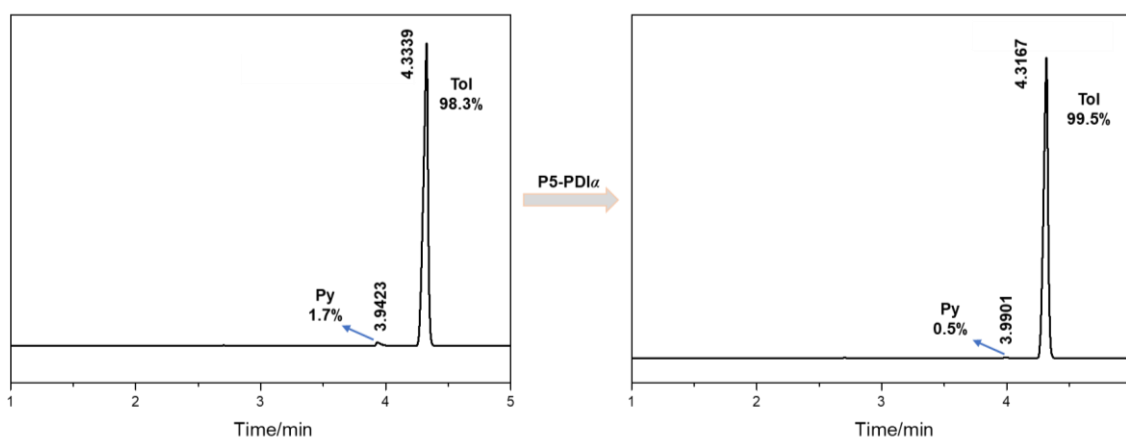


**Figure S27.** Relative Py and Tol uptake in  $\text{P5-PDI}\alpha$  after adsorption of the Tol/Py mixtures ( $v:v = 98:2$ ).

For the Tol purification experiment, an open 5.00 mL vial containing 50.00 mg of guest-free  $\text{P5-PDI}\alpha$  adsorbent was placed in a sealed 20.00 mL vial containing 100  $\mu\text{L}$  of Tol and Py mixtures. The mixture ratios were approximately 98:2. The purity of Tol before and after adsorption were measured by GC.

## 7. References

---

- (S1) T. Ogoshi, S. Kanai, S. Fujinami, T.-a. Yamagishi and Y. Nakamoto, *para*-Bridged symmetrical pillar[5]arenes: their lewis acid catalyzed synthesis and host–guest property. *J. Am. Chem. Soc.* **2008**, *130*, 5022.
- (S2) S. De and S. Ramakrishnan, *Macromolecules* **2009**, *42*, 8599.
- (S3) G. M. Sheldrick, Crystal structure refinement with SHELXL. *Acta Crystallogr. C.* **2015**, *71*, 3.
- (S4) O. V. Dolomanov, L. J. Bourhis, R. J. Gildea, J. A. K. Howard and H. Puschmann, *OLEX2*: a complete structure solution, refinement and analysis program. *J. Appl. Cryst.* **2009**, *42*, 339.